Desalination and Water Treatment
www.deswater.com

doi: 10.5004/dwt.2018.22021

105 (2018) 322–331
February

Equilibrium isotherms, kinetics, and thermodynamics studies of methylene blue adsorption on pomegranate (*Punica granatum*) peels as a natural low-cost biosorbent

Ali H. Jawad[a,*], Azal Shakir Waheeb[b], Ramlah Abd Rashid[a], Wan Izhan Nawawi[c,d], Emad Yousif[e]

[a]*School of Chemistry and Environment, Faculty of Applied Sciences, Universiti Teknologi MARA, 40450 Shah Alam, Selangor, Malaysia, Tel. +603-55211721, email: ahjm72@gmail.com, ali288@salam.uitm.edu.my (A.H. Jawad), Tel. +6012-4872038, email: ramlahabdrashid@yahoo.com (R.A. Rashid)*
[b]*Chemistry Department, College of Science, Al-Muthanna University, Al-Muthanna, Iraq, Tel. +9647830791852, email: azilshaker70@gmail.com (A.S. Waheeb)*
[c]*Faculty of Applied Sciences Universiti Teknologi MARA, 02600 Arau, Perlis, Malaysia, Tel. +6049882305, email: wi_nawawi@perlis.uitm.edu.my (W.I. Nawawi)*
[d]*Department of Chemistry, University of York, Heslington, York, YO10 5DD, UK*
[e]*Department of Chemistry, College of Science, Al-Nahrain University, Baghdad, Iraq, Tel. +9647705839300, email: emad_yousif@hotmail.com (E. Yousif)*

Received 30 May 2017; Accepted 12 February 2018

ABSTRACT

In this work, the potential of biomass waste, pomegranate (*Punica granatum*) peel (PP) as low cost adsorbent for adsorption of methylene blue (MB) from aqueous solution was studied. The physicochemical properties of PP were characterized using instrumental analyses such as CHNS-O analyzer, Brunauer-Emmett-Teller (BET), Fourier transform infrared spectroscopy (FTIR), scanning electron microscopy (SEM), and point of zero charge (pH_{pzc}) analysis. Batch mode adsorption studies were conducted by varying operational parameters such as adsorbent dosage (0.02–0.16 g), solution pH 3–11, initial MB concentrations (50–300 mg/L), and contact time (0–390 min). The equilibrium data was found to better fit with Langmuir isotherm model compare to Freundlich model. The maximum adsorption capacity, q_{max} of PP for MB was 200 mg/g at 303 K. The kinetic study revealed that the present system obeyed pseudo-second-order (PSO) model. The thermodynamic adsorption parameters, standard enthalpy ($\Delta H°$), standard entropy ($\Delta S°$), and standard free energy ($\Delta G°$) showed that the adsorption of MB onto PP surface exothermic and spontaneous under the experimented conditions. All results mentioned above indicate that the PP can feasibly employ for the elimination of MB from aqueous solution.

Keywords: Adsorption; Methylene blue; Pomegranate peels; Biomass waste; Low-cost adsorbent

1. Introduction

Industries such as paints, plastics, papers, leathers, and textile release dyes contained effluents caused a serious environmental issue due to their injurious impacts upon aquatic organisms and human beings. The released of dyes into water body without suitable treatment will give water disagreeable color and considered source of non-aesthetic pollution and eutrophication, toxic and potentially carcinogenic due to their complex aromatic structures and synthetic nature [1]. Methylene blue (MB) is one of the most common basic dyes for dyeing cotton, silk, and wool. It has been recognized to cause a number of adverse health effects, for example breathing difficulties, eye burns, allergy, profuse

*Corresponding author.

sweating, nausea, vomiting, mental confusion, jaundice and even dysfunction of brain, kidney, liver, reproductive and central nervous system [2]. Hence, the treatment of effluent containing MB is highly required due to its dangerous impacts on ecosystem.

Government regulation requires wastewater to be treated, thus there is a need to have an effective process that can efficiently remove dyes [3]. Several of chemical, physical, and biological procedures for dyes removal from aqueous solutions have been testified in the past years including electrochemical treatment [4], membrane filtration [5], Fenton chemical oxidation [6], and photocatalysis [7–12]. Despite the availability of mentioned methods, adsorption process remain as the most predominant methods used in wastewater treatment due to its effectiveness, simplicity, flexibility, and ease of implementation without producing hazardous secondary products [13–15].

Activated carbon is one of the most common adsorbent used for removal of dyes, nevertheless due to a high operational cost, and extremely difficult for regeneration [16], limits its application in huge scale. Taking these criteria into consideration, there is an interest to search for economic and efficient techniques using alternative materials such as natural and vegetal adsorbent [17–19]. Biomass wastes has been completely utilized as a precursor in adsorption process since it has been recognized as the most affordable and achievable choice for removal of dyes. The past few years have seen the successful applications of fruit peels such as orange peel [20–21], mango peel [22], pomelo peel [23], grapefruit peel [24], lemon peel [25], banana peel [21,26,27], jackfruit peel [28], durian peel [29] and passion fruit peel [30,31] for removing dyes from aqueous solution via adsorption process.

Agricultural waste peels have been considered as an ecological burden for the society. Anyhow, waste peels, as lignocellulosic biomass-rich materials, have stimulated new gateways for the production of renewable, low cost and sustainable adsorbents for water treatment applications. Fruit and vegetable peels consist of the highest percentage of wastes in most kitchen garbage bins. Furthermore, in fruit and vegetable industries, it is common that some waste is generated during processing (selecting, sorting, boiling processes) [32]. Processing of fruits and vegetables produces different types of waste including a solid waste of peel/skin. Plenty of the fruits and vegetables skins (peels) are discarded in the garbage. Fruits and vegetables wastes and by-products, which are formed in great amounts during industrial processing, represent a serious problem, as they exert an influence on environment and need to be managed and/or utilized [32].

Pomegranate or its scientific name, *Punica granatum* is one of the famous fruit in the world due to its delicious taste as well as rich with nutrition. It consists of edible part, seed, and peel. Pomegranate peel (PP) is a by-product from pomegranate juice, hence it can be considered as waste which owns no commercial value. Research conducted by Moghadam et al. [33] stated that the PP constitutes from 5 to 15% of its total weight. This present work investigates the use of PP as potential low-cost adsorbent for the removal of MB from aqueous solution via batch mode adsorption studies. Batch mode adsorption experiments were conducted by manipulating operational parameters such as adsorbent dosage, solution pH, initial MB concentration, contact time, and temperature. The equilibrium adsorption data were fitted to Langmuir and Freundlich isotherm models while kinetic data were fitted to pseudo-first-order and pseudo-second-order models. The thermodynamic profiles of MB adsorption by PP were also evaluated. The physicochemical properties of PP before and after MB adsorption were studied to understand the adsorption behavior of MB onto PP surface.

2. Materials and methods

2.1. Adsorbate (MB)

Methylene blue (MB) attained from R&M Chemicals, Malaysia was applied as an adsorbate. All MB solutions were prepared and diluted with ultra-pure water. The used MB has a chemical formula of $C_{16}H_{18}Cl_3S{\cdot}xH_2O$ with molecular weight of 319.86 g/mol.

2.2. Preparation of PP as adsorbent

The pomegranate peels (PP) were obtained from a local fresh juice shop in Penang, Malaysia. PP was firstly washed with distilled water and then dried at 105°C in the oven for 24 h to remove the moisture contents. The dried PP was subsequently ground and sieved to the size of 1–2 mm. The ultimate elemental analysis of PP was accomplished using a CHNS-O analyzer (Perkin-Elmer, Series II, 2400). The total surface area of PP was analyzed using BET method (Quantachrome Corporation, USA). The functional groups of PP before and after MB were studied via Fourier Transform infrared (FTIR) spectroscopy (Perkin Elmer, Spectrum RX I) in transmission mode with a spectral range from 4000 cm^{-1} to 400 cm^{-1} with a resolution of 4 cm^{-1}. All samples were prepared with spectroscopic grade KBR which comprises ~ 80% (w/w) of the total sample and were evaluated in the form of finely ground powders. The surface morphology of PP before and after adsorption of MB was observed using a scanning electron microscope (SEM; FESEM CARL ZEISS, SUPKA 40 VP). The pH at the point-of-zero charge (pH_{pzc}) was estimated by the solid addition technique by using a pH meter (Metrohm, Model 827 pH Lab, Switzerland), as described by Lopez-Ramon et al. [34]. In this method, the pH of a suspension of the PP (0.08 g) in a NaCl aqueous solution (100 mL at 0.01 mol/L) was adjusted to successive initial values between 3 and 11. The suspensions were agitated 24 h and the final pH was measured and plotted against the initial pH. The pH_{pzc} was determined at the value at which $pH_{final} - pH_{initial}$.

2.3. Batch mode adsorption experiments

The batch mode adsorption experiments of MB onto PP were carried out in a series of 250 mL Erlenmeyer flasks containing 100 mL of MB solution. The flasks were capped and agitated in an isothermal water bath shaker (Memmert waterbath, model WNB7-45, Germany) at fixed shaking speed of 120 stroke min^{-1} and 303 K until equilibrium was achieved. Batch mode adsorption experiments were performed by changing operational parameters such as

adsorbent dosage (0.02–0.16 g), solution pH (3–11), initial MB concentration (50–300 mg/L), and contact time (0–390 min) to determine the optimum uptake conditions for MB adsorption. The pH of MB solution was adjusted by adding either 0.10 M HCl or NaOH. For the quantification of the adsorbed MB, the supernatant of the PP-MB mixture was collected with a 0.20 µm nylon syringe filter and the concentrations of MB were monitored at different time interval using a HACH DR 2800 Direct Reading Spectrophotometer at the maximum wavelength (λ_{max}) of absorption at 661 nm. In the thermodynamic study, similar procedures were applied at 313 and 323 K, with the other parameters held constant. Blanks tests were carried out to account for the color leached by the adsorbent and adsorbed by the glass containers, in which blank runs with only the adsorbents in 100 mL of ultra-pure water and 100 mL of MB solution without any adsorbent were conducted concurrently at similar conditions. The adsorption capacity at equilibrium, q_e (mg g^{-1}) and the percentage of color removal, R_c (%) of MB were calculated using Eqs. (1) and (2):

$$q_e = \frac{C_o - C_e}{W} V \quad (1)$$

$$R_c(\%) = \frac{C_o - C_e}{C_o} \times 100 \quad (2)$$

C_o is the initial MB concentration (mg/L); C_e is the MB concentration at equilibrium (mg/L); V is the volume of MB solution (L); and W is the dry mass of adsorbent PP (mg). Adsorption experiments were conducted in triplicate under identical conditions and the results are reported as an average value.

Table 1
Comparison of ultimate analysis of PP with other biomass materials

Biomass material	Ultimate analysis (wt. %)					Reference
	C	H	N	O	S	
Pomegranate peels (PP)	43.95	5.46	0.14	50.45*	ND	This work
Orange peel	39.8	5.9	0.8	46.9	ND	[20]
Almond peel	45.5	5.8	0.8	45.7	ND	[20]
Garlic peel	37.01	4.22	1.04	47.71	0.81	[35]
Green pea peels	61.74	1.37	5.63	21.93	9.33	[36]
Cassava stalk	51.12	6.87	0.67	41.34	<0.1	[37]
Cassava rhizome	51.59	6.69	1.27	40.45	<0.1	[37]
Sugarcane	43.74	6.30	0.44	42.42	ND	[38]
Banana Leaves	43.28	6.23	0.98	49.02	0.49	[39]
Banana Pseudo-stem	37.93	4.46	1.87	55.37	0.37	[40]
Banana FBS	35.58	4.62	2.19	57.16	0.45	[40]

*by difference
ND: Not detected

Table 2
Textural properties of PP

Properties	
Micropore area (m^2/g)	0.3439
Mesopore area (m^2/g)	0.6757
BET surface area (m^2/g)	1.0196

3. Results and discussion

3.1. Characterization of PP

The ultimate elemental analysis of PP was compared with other biomass materials and tabulated in Table 1. The result indicates that carbon and oxygen are the major constituents of PP along with measurable amount of hydrogen and nitrogen. Table 2 summarizes the textural properties of PP. It is learnt that, the total surface area of PP was low with almost 66.00% of the surface area was dominated by mesoporous structure. The pattern of adsorption onto biomass materials is highly associated to the availability of the active functional groups and bonds of the PP surface. For the elucidation of these active sites, FTIR spectroscopy was performed upon the PP before and after MB adsorption. Several IR bands appearing in the FTIR spectrum of PP before adsorption (Fig. 1a) that signified various functional groups, in accordance with their respective wavenumber (cm^{-1}) position, are as reported in the literature [41]. The broad and intense band around 3400 cm^{-1} is attributed by the –OH stretching vibrations of cellulose, pectin and lignin while the band at 2900 cm^{-1} corresponds to the –CH stretching vibrations of methyl group. The asymmetric and symmetric vibrations of –COO of the ionic carboxylic groups within PP are represented by the band at 1600. The IR bands around 1000 cm^{-1} region is assigned to the C-O and C-O-C stretching vibrations in carboxylic acids, alcohols, phenols or ester groups. As depicted by the IR spectral of PP after MB adsorption (Fig. 1b), new bands assigned to anhydride (1600–1700 cm^{-1}) and nitro (1370–1380 cm^{-1}) are attributed to MB [16]. Furthermore, some of the bands shifted and became more pronounced suggest the interaction of MB molecules with the functional groups of PP has taken place. Therefore, it can be conclude that the IR spectral of PP before MB adsorption strongly shows that the external surface of PP is rich in carboxylic and hydroxyl groups, which can be deprotonated to bind the positively charged MB. The changes in the surface morphology of PP before and after MB adsorption were determined by comparing their SEM images. Based on Fig. 2a, the PP before MB adsorption possesses uneven and irregular surface with considerable layers of rough heterogeneous pores which offers high probability for dye molecules to be adsorbed [42]. Meanwhile, the SEM image of PP after MB adsorption in Fig. 2b reveals smoother surface features with obvious reduced pore structures, indicating the uptake and entrapment of MB molecules by the accessible pore vicinities of the PP surface. Fig. 2b proves the engagement of MB onto PP and this may be related to the presence of carboxylic and hydroxyl groups within PP, as evidenced by the IR spectral (Fig. 1) discussed earlier on, which act as active sites for the adsorption of MB molecules. The pH_{pzc} of PP was determined to find out the pH at which the electrical charge of the surface of PP was zero. Fig. 3 shows that the pH_{pzc} of PP was at pH 5.4 which reflected the acidity of PP, in agreement

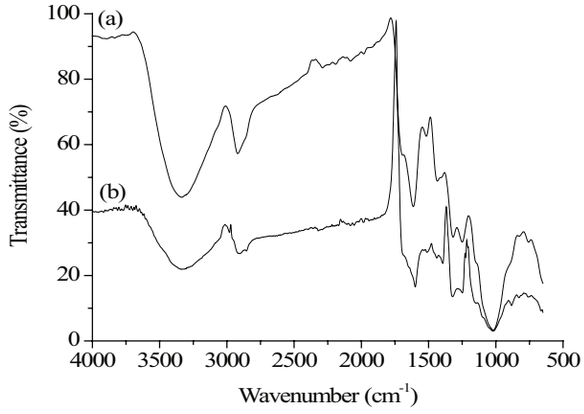

Fig. 1. FT-IR spectra of PP: (a) before MB adsorption (b) after MB adsorption.

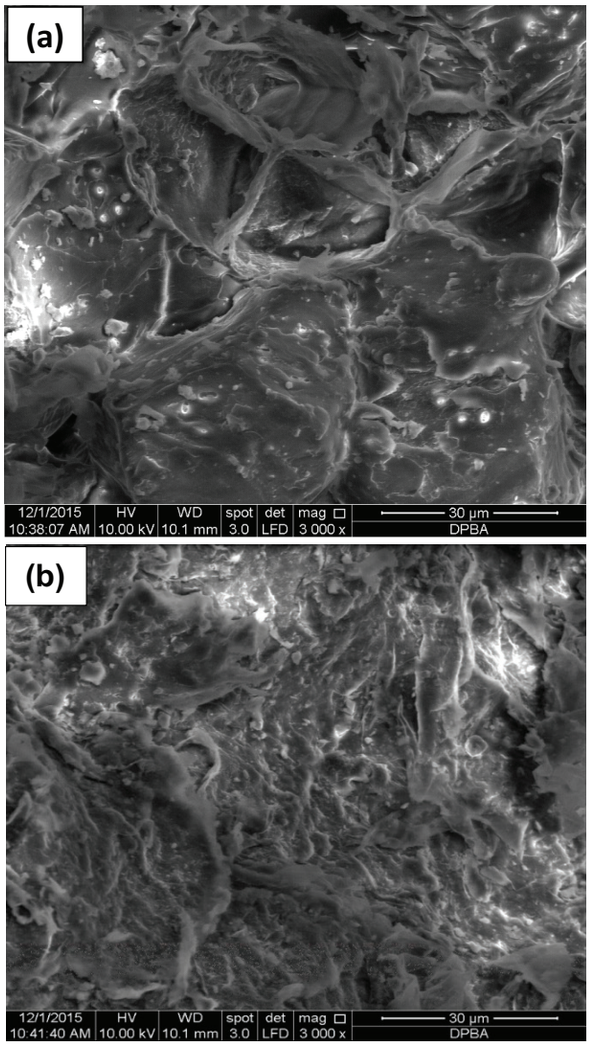

Fig. 2. Typical SEM micrograph of PP particle (3,000 magnifications): (a) before MB adsorption and (b) after MB adsorption.

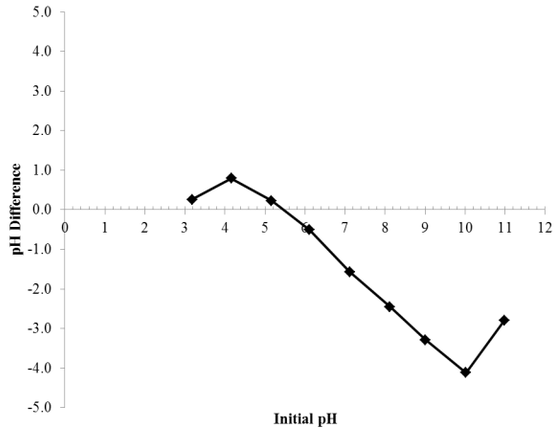

Fig. 3. pH_{pzc} of PP suspensions.

with the above-mentioned IR results (Fig. 1) that carboxylic acids are present in abundance within PP. Adsorption of anions is favored at solution pH below the pH_{pzc} value as the surface of PP is positively charged due to protonation whereas at solution pH above the pH_{pzc} value, the surface of PP becomes negatively charged and thus, adsorption of cations is preferred. In this regard, it is predicted that the adsorption of the cationic MB by PP will be appropriate at solution pHs above 5.4 because of electrostatic interactions.

3.2. Batch mode adsorption of MB

3.2.1. Effect of adsorbent dosage

To study the influence of adsorbent dosage on MB adsorption onto the surface of PP, the experiment was conducted by varying amount of PP, ranging from 0.02 to 0.16 g at fixed MB volume of 100 mL and initial dye solution, C_o, of 100 mg/L. Throughout the experiment, temperature was kept constant at 303 K, shaking speed of 120 stroke min^{-}, contact time of 60 min and an unadjusted pH value of 5.6 for the initial MB solution. The result in Fig. 4 shows the effect of PP dosage on the removal of MB. In general, the percentage removal of dyes increased with adsorbent dosage due to the increase in the total available surface area and the number of adsorption sites on the adsorbent surface allowed more bindings of dye molecules [28]. In this study, the removal MB increased correspondingly with the PP dosage until 0.08 g with 82.47% removal, but further addition rendered no significant impact on the MB removal percentage. This can be seen from a nearly constant percentage removal obtained at higher PP dosages. This outcome could be caused by the accumulation of PP particles at higher dosages which led to decrease in the effective surface area of PP for MB uptake. Therefore, 0.08 g of PP was selected for the following experiments.

3.2.2. Effect of pH

The pH value of the solution, which influences the surface charge of the adsorbent and the speciation magnitude of dye, plays an important role in controlling the adsorp-

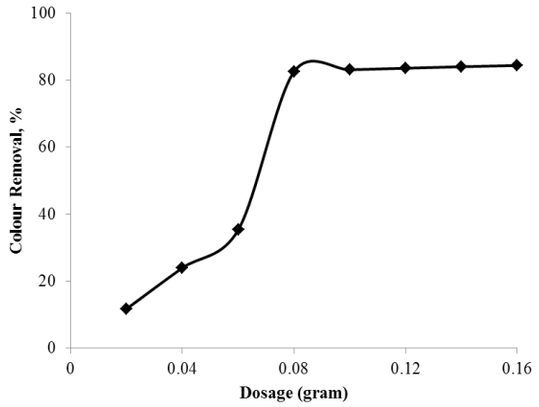

Fig. 4. Effect of PP dosage on MB removal (%) at $[MB]_o$ = 100 mg/L, V = 100 mL, pH = 5.60, T = 303 K, shaking speed = 120 stroke/min and contact time = 60 min.

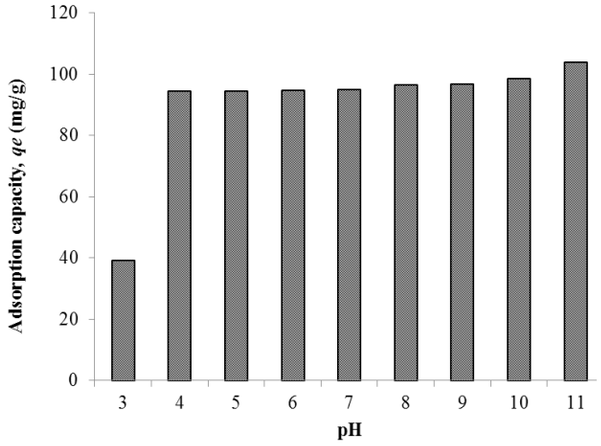

Fig. 5. Effect of pH on the adsorption capacity of MB by PP at $[MB]_o$ = 100 mg/L, V = 100 mL, T = 303 K, shaking speed = 120 stroke/min, contact time = 60 min and PP dosage = 0.08 g.

tion process. Fig. 5 shows the effect of pH on the adsorption of MB by PP. As observed, the adsorption of MB by PP increased steadily with the increasing solution pH up to pH 4.0, later, further increase in pH values demonstrated no significant changes. Lower value of adsorption capacity at acidic pH may be either due to excess concentration of H^+ ions competing with the MB dye cations for adsorption sites. Moreover, at solution pH < pH_{pzc} = 5.4, the surface of PP was essentially positively charged and thus, repulsion between the MB cations and the PP may have occurred and decreased the MB adsorption capacity. On the other hand, as the pH of the process increased, the surface of PP was likely to adopt negative surface charges and became increasingly favorable for MB adsorption due to electrostatic forces of attraction. The adsorption of MB remained almost constant from pH 4.0 onwards may be due to the complete deprotonation of the active group, i.e. $COOH \rightarrow COO^-$ of PP surface when the solution pH surpassed 5 [43]. Thus, the best solution pH for the removal of MB by PP was at between pH 4.0 to 10.0. Since the unadjusted pH of the initial MB solution (5.6) lies within the optimal pH range and in order to lessen chemical and time consumptions, further experiments on the adsorption of MB by PP were conducted at pH 5.6.

3.2.3. Effect of initial dye concentration and contact time

The adsorption efficiency of MB adsorption onto PP surface was evaluated as a function of initial dye concentration and contact time as elucidated in Fig. 6. The MB adsorption profiles at all concentrations shows that the adsorption process at initial stage was rapid at the beginning and gradually decreased as time proceeded to equilibrium. This is because, at the initial stage of the adsorption process, there were more unoccupied adsorption sites of PP available for the uptake of MB molecules and as the time lapsed, the availability of the sites became inadequate which led to the slowing down of the process. Based on this work, 50 mg/L of MB took about 120 min to reach the adsorption equilibrium state while MB with concentration of 300 mg/L required almost 390 min. This observation can be clarified by the facts that in the adsorption process, initially the dye

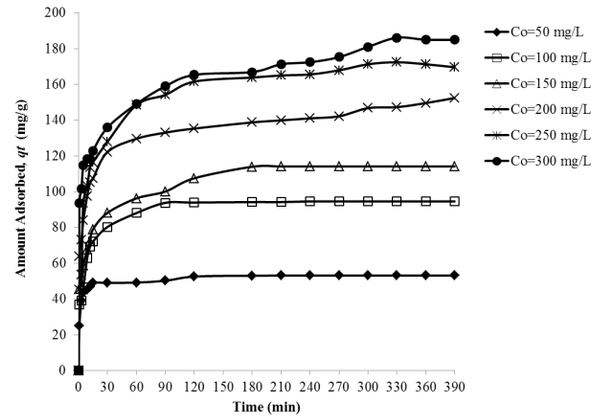

Fig. 6. Effects of initial concentration and contact time on the adsorption of MB by PP (V = 200 mL, T = 303 K, pH = 5.6, shaking speed = 120 stroke/min and PP dosage = 0.16 g).

molecules need to encounter the boundary layer effect and then diffuse from the boundary layer film onto adsorbent surface and then finally, diffuse into the porous structure of the adsorbent [44]. Therefore, MB solutions with higher initial concentrations will take longer time to approach equilibrium due to greater amount of dye molecules as well as the tendency MB molecules to penetrate deeper into the porous interior of the adsorbent [29]. The amount of MB adsorbed by PP at equilibrium improved significantly from 53.06 to 184.93 mg/g as the initial concentration of MB was increased from 50 to 300 mg/L. It is shown that initial dye concentration plays a significant role in the adsorption capacity of MB by PP.

3.3. Adsorption isotherm studies

The interaction between adsorbent and adsorbate can be determined by isotherm study. In this paper, the adsorption equilibrium data of MB onto PP surface was calculated

using Langmuir and Freundlich isotherm models. The quality of the fit was evaluated by comparing the coefficient of determination, R^2 values. The Langmuir isotherm model describe that adsorption sites at the adsorbent are fundamentally homogeneous based the assumption that monolayer adsorption take place on uniformly energetic adsorption site with no interaction between adsorbate molecules on adjacent sites [45]. The adsorbent has the finite adsorption capacity in which no further adsorption can occur once a molecule occupied a site and reached an equilibrium saturation point [46]. The linear mathematical expression of Langmuir isotherm is represented by Eq. (3):

$$\frac{C_e}{q_e} = \frac{1}{q_m K_L} + \frac{1}{q_m} C_e \tag{3}$$

where C_e is the equilibrium concentration (mg/L) and q_e is the amount of adsorbed species per specified amount of adsorbent (mg/g) while K_L (L/mg) and q_m (mg/g) are the Langmuir constants associated to the adsorption affinity and capacity, respectively. Thus, a plot of C_e/q_e vs. C_e should yield a straight line with a slope $(1/q_m)$ and intercept $(1/q_m K_L)$ as shown in Fig. 7(a). In contrast, the Freundlich model is based on the assumption that adsorption occurs on heterogeneous surfaces with non-uniform distribution of adsorption energy. This model is employed to describe multilayer adsorption with interaction between the adsorbate molecules and is not limited to monolayer formation of adsorbate molecules on the adsorbent [47]. The linear mathematical form of Freundlich isotherm is shown by Eq. (4):

$$\ln q_e = \ln K_F + \frac{1}{n} \ln C_e \tag{4}$$

where K_F [mg/g (L/mg)$^{1/n}$] and $1/n$ are the Freundlich isotherm constants related to the adsorption capacity and intensity, respectively. The K_F and n values can be derived from the intercept and slope of the ln q_e vs. ln C_e plot given in Fig. 7b. The adsorption parameters for both the isotherm models are listed in Table 3. The MB adsorption equilibrium data agreed satisfactory with Langmuir model since the R^2 value is greater as compared to the Freundlich model. The dimensionless separation factor, R_L, associated to Langmuir isotherm can be obtained to evaluate the feasibility of the adsorption on the adsorbent [48] by using Eq. (5):

$$R_L = \frac{1}{1 + K_L C_o} \tag{5}$$

where C_o refers to the initial concentration of the adsorbate. The value of R_L indicates the adsorption process to be either irreversible ($R_L = 0$), favorable ($0 < R_L < 1$), linear ($R_L = 1$) or unfavorable ($R_L > 1$). The calculated R_L values at different MB concentrations are listed in Table 4. The obtained R_L values are in the range of 0–1 for all initial concentrations, indicating that the adsorption of MB onto PP is a favorable process. The R_L values gradually decrease as the concentrations were increased; showing that higher initial concentration of MB may improve the adsorption process [49]. Based on the Freundlich isotherm model, the slope, $1/n$ ranging between 0 and 1, is a measure of surface heterogeneity, whereby the surface is more heterogeneous as the $1/n$ value approaches zero. A value of $1/n < 1$ indicates a normal Langmuir isotherm while $1/n >$ is reflective of cooperative adsorption [50]. Moreover, the value of exponent $n > 1$ is an implication of a favorable adsorption process. In this case, the obtained $1/n$ value for PP is below unity, indicating that the favorable MB adsorption process and reconfirmed a normal Langmuir isotherm characteristic. These results acknowledged that the surface binding sites of PP are homogeneous in nature whereby each MB is attached

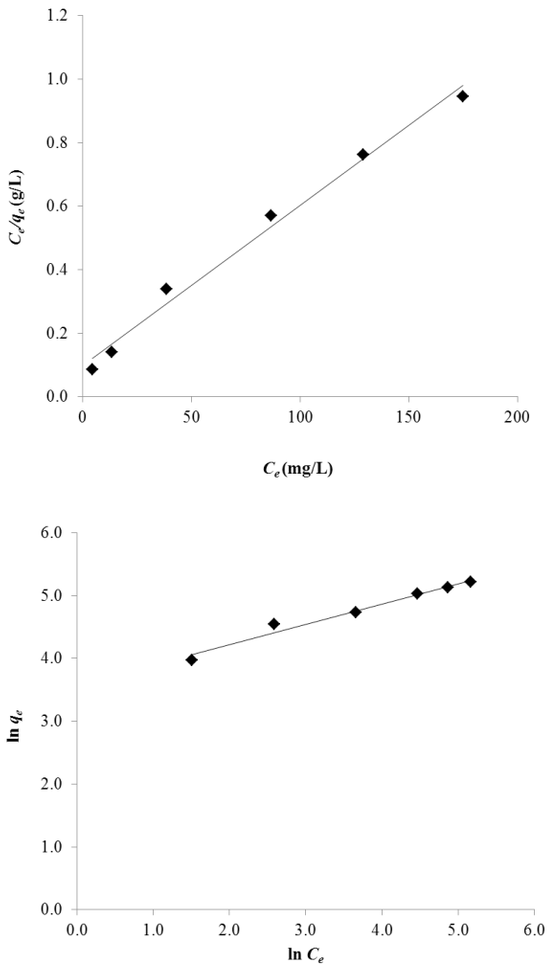

Fig. 7. Isotherm models for the adsorption of MB onto PP: (a) Langmuir (b) Freundlich.

Table 3
Isotherm parameters for adsorption of MB by PP.

Langmuir isotherm		
q_m (mg/g)	K_L (L/mg)	R^2
200	0.05	0.989
Freundlich isotherm		
K_F [(mg/g) (L/mg)$^{1/n}$]	$1/n$	R^2
35.60	0.32	0.974

Table 4
Dimensionless constant separation factor, R_L for adsorption of MB onto PP at various initial concentrations.

[MB] (mg/L)	R_L
50	0.286
100	0.167
150	0.118
200	0.091
250	0.074
300	0.063

with similar adsorption energy. The results show that the formation of a surface monolayer of MB molecules for PP, in which the monolayer adsorption capacity, q_m for PP towards MB was compared against that of the other types of fruit peels in Table 5. Therefore, the PP utilized in this study is an effective biosorbent for removal of cationic dye like MB from aqueous solution.

3.4. Adsorption kinetic studies

The adsorption kinetic of MB into PP surface data were analyzed using pseudo-first-order (PFO) and pseudo-second-order (PSO) models to determine the adsorption rate as well as to explain the interaction between adsorbent and adsorbate that occurred. The conformity between the experimental data and the model predicted values was presented by the coefficient of determination, R^2 values. The PFO is constructed based on the prediction that the change of adsorbate uptake rate with time is proportional to the difference in concentration at equilibrium and the amount of adsorbed adsorbate with time [51] and is expressed as Eq. (6):

$$\ln\left(q_e - q_t\right) = \ln\left(q_e\right) - k_1 t \tag{6}$$

where q_e (mg/g) and qt (mg/g) are the amount of adsorbate adsorbed onto adsorbent at equilibrium and time t, respectively, while k_1 is the PFO rate constant. The k_1 values can be determined from the slope of the plot of $\ln(q_e - q_t)$ vs. t shown in Fig. 8a. Meanwhile, the PSO is based on the assumption that the rate-limiting step of the adsorption process may be chemisorption involving sharing or exchange of electrons between adsorbent and adsorbate [52]. The linear form of the PSO model is described by Eq. (7):

$$\frac{t}{q_t} = \frac{1}{k_2 q_e^2} + \frac{t}{q_e} \tag{7}$$

where k_2 (g/min mg) is the PSO rate constant. The k_2 and theoretical $q_{e,cal}$ values can be calculated from the intercept and slope of the t/q_t vs. t plot depicted in Fig. 8b. The kinetic data for the adsorption of MB onto PP were calculated from the related plots and are tabulated in Table 6. The presented data shows that the MB adsorption kinetic data was better fitted by the PSO model with R^2 values of ≥ 0.997 for all tested concentrations. This result infers that the rate of MB adsorption onto PP seemed to be governed by chemi-

Table 5
Comparison of adsorption capacities for MB by different untreated fruit peels adsorbents

Fruit peels adsorbents	Adsorbent dosage (g)	Adsorption capacity, q_m	References
Orange peel	0.10 g/100 mL	218 mg/g	[20]
Almond peel	0.10 g/100 mL	208 mg/g	[20]
Orange peel	0.10 g/100 mL	18.60 mg/g	[21]
Banana peel	0.10 g/100 mL	20.80 mg/g	[21]
Pomelo peel	0.40 g/100 mL	133 mg/g	[23]
Banana peel	1 g/1000 mL	18.65 mg/g	[26]
Banana peel powder	0.10 g/100 mL	111.11 mg/g	[27]
Jackfruit peel	0.60 g/200 mL	285.71 mg/g	[28]
Yellow passion fruit peel	1 g/50 mL	0.0068 mmol/g	[30]
Yellow passion fruit peel	1g/100 mL	44.7 mg/g	[31]
Pomegranate peel	0.08 g/ 100 mL	200 mg/g	This work

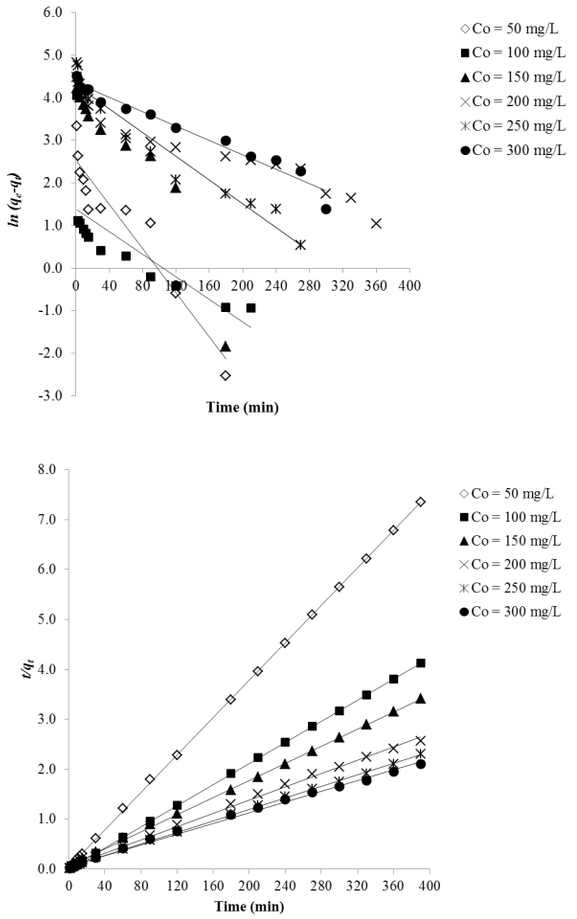

Fig. 8. Kinetic profiles for the adsorption of MB onto PP: (a) pseudo-first order (b) pseudo-second order.

Table 6
PFO and PSO kinetic parameters and their corresponding values at different initial dye concentrations by PP

	Concentration (mg/L)					
	50	100	150	200	250	300
$q_{e,exp}$ (mg/g)	53.06	94.56	114.06	152.40	169.52	184.93
PFO						
$q_{e,cal}$ (mg/g)	12.48	3.99	71.97	55.56	73.85	76.88
k_1 (1/m)	0.026	0.013	0.028	0.075	0.014	0.008
R^2	0.896	0.544	0.896	0.924	0.946	0.967
PSO						
$q_{e,cal}$ (mg/g)	53.19	94.34	116.28	149.25	172.41	185.18
k_2 (g/mg min)	0.009	0.02	0.001	0.001	0.001	0.001
R^2	0.999	1.0000	0.999	0.999	0.999	0.997

cal process that involved sharing of electrons or by covalent forces through exchanging of electrons between adsorbent and adsorbate. Similar finding was obtained for adsorption of MB onto orange peel [20], and jackfruit peel [28].

3.5. Adsorption thermodynamics studies

The thermodynamic parameters of adsorption of MB onto PP were derived from the experimental data obtained at 303, 313 and 323 K to assume the nature and thermodynamic feasibility of the adsorption process. The standard free energy change (Δ*G*°), enthalpy change (Δ*H*°) and entropy change (Δ*S*°) related to the adsorption processes are calculated using Eqs. (8), (9) and (10):

$$k_d = \frac{q_e}{C_e} \tag{8}$$

$$\Delta G^\circ = -RT \ln k_d \tag{9}$$

$$\ln k_d = \frac{\Delta S^\circ}{R} - \frac{\Delta H^\circ}{RT} \tag{10}$$

where k_d is the distribution coefficient, q_e is the concentration of MB adsorbed onto PP at equilibrium (mg/L), C_e is the equilibrium of MB in the liquid phase (mg/L), R is the universal gas constant (8.314 J/mol K), and T is the absolute temperature (K). The values of Δ*H*° and Δ*S*° were calculated from the slope and intercept of Van't Hoff plot (ln k_d vs. 1/T) given in Fig. 9 and the values of the parameters are listed in Table 7. As the adsorption temperature increased, the MB adsorption capacity of PP decreased and this suggested that the adsorption process was exothermic in nature. The observation can be attributed to the weakening of bonds between the adsorbate molecules and active sites of adsorbents at high temperatures [53]. The negative Δ*G*° values supported that the adsorption process was spontaneous and more favorable at low temperature. Negative value of Δ*H*° (–5.97 kJ/mol) confirmed the exothermic nature of the adsorption process and the negative Δ*S*° (–3.54 J/mol K) value revealed the decrease in the randomness at solid-solution interface. There is unequal release of energy during the adsorption process and the magnitude of Δ*H*° value offers information about the forces that governed the adsorption process. The energy (Δ*H*°) related to physical forces: van der Waals (4–10 kJ/mol), hydrophobic interaction (5 kJ/mol), hydrogen bonding (2–40 kJ/mol), coordination exchange (40 kJ/mol), dipole bond forces (2–29 kJ/mol) and electrostatic interaction (20–80 kJ/mol) while for chemical forces (>60 kJ/mol) [54]. In this work, the ΔH° value was found 5.97 kJ/mol, confirming that physical forces were involved in the adsorption of MB onto PP.

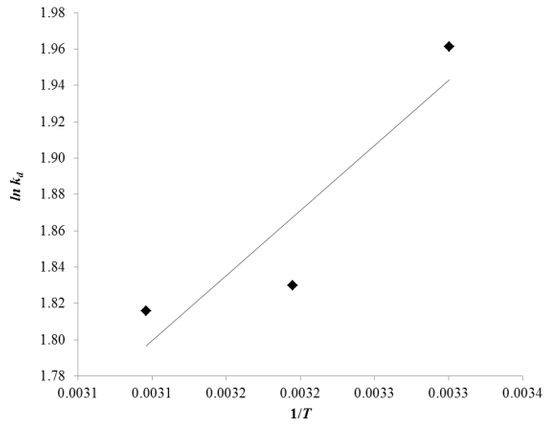

Fig. 8. Kinetic profiles for the adsorption of MB onto PP: (a) pseudo-first order (b) pseudo-second order.

Table 7
Thermodynamic parameters values for the adsorption of MB onto PP

Temperature (K)	Thermodynamics Parameters			
	k_d	ΔG° (kJ/mol)	ΔH° (kJ/mol)	ΔS° (J/mol K)
303	7.11	–4.89	–5.97	–3.54
313	6.23	–4.86		
323	6.15	–4.82		

4. Conclusion

The biomass waste PP exhibited great potential as low-cost adsorbent for effective removal of MB from aqueous solution. Physicochemical characterizations revealed that the carboxyl and hydroxyl groups of PP play important role in the adsorption of MB. The optimum PP dosage was 0.08 g and superior MB adsorption capacity was obtained in solution pH 5.6. The adsorption capacity increased with increasing MB concentrations. The adsorption equilibrium data obeyed the Langmuir isotherm model and the monolayer adsorption capacity, q_{max} was found to be 200 mg/g. Meanwhile, the PSO model was determined to be better fit for kinetic model compared to the PFO model. The thermodynamic parameters values showed that the MB adsorption by PP was spontaneous and exothermic in nature.

Acknowledgement

We gratefully acknowledge Universiti Teknologi MARA, Faculty of Applied Sciences, School of Chemistry and Environment for facilitating this work.

References

[1] A.H. Jawad, M.A. Islam, B.H. Hameed, Cross-linked chitosan thin film coated onto glass plate as an effective adsorbent for adsorption of reactive orange 16, Int. J. Biol. Macromol., 95 (2017) 743–749.
[2] M. Rafatullah, O. Sulaiman, R. Hashim, A. Ahmad, Adsorption of methylene blue on low-cost adsorbents: A review, J. Hazard Mater., 177 (2010) 70–80.
[3] N.S.A. Mubarak, A.H. Jawad, W.I. Nawawi, Equilibrium, kinetic and thermodynamic studies of Reactive Red 120 dye adsorption by chitosan beads from aqueous solution, Energ. Ecol. Environ., 2(1) (2017) 85–93.
[4] M. Panizza, A. Barbucci, R. Ricotti, G. Cerisola, Electrochemical degradation of methylene blue, Sep. Purif. Technol., 54(3) (2007) 382–387.
[5] M. Bielska, J. Szymanowski, Removal of methylene blue from waste water using micellar enhanced ultrafiltration, Water Res., 40(5) (2006) 1027–1033.
[6] L. Shen, P. Yan, X. Guo, H. Wei, X. Zheng, Three-dimensional electro-Fenton degradation of methylene blue based on the composite particle electrodes of carbon nanotubes and nano-Fe_3O_4, Arab J. Sci. Eng., 39(9) (2014) 6659–6664.
[7] A.H. Jawad, A.F.M. Alkarkhi, N.S.A. Mubarak, Photocatalytic decolorization of methylene blue by an immobilized TiO_2 film under visible light irradiation: optimization using response surface methodology (RSM), Desal. Water Treat., 56(1) (2015) 161–172.
[8] A.H. Jawad, N.S.A. Mubarak, M.A.M. Ishak, K. Ismail, W.I. Nawawi, Kinetics of photocatalytic decolourization of cationic dye using porous TiO_2 film, J. Taibah Univ. Sci., 10(3) (2016) 352–362.
[9] W.I.N.W. Ismail, S.K. Ain, R. Zaharudin, A.H. Jawad, M.A.M. Ishak, K. Ismail, S. Sahid, New TiO_2/DSAT immobilization system for photodegradation of anionic and cationic dyes, Int. J. Photoenergy, 6 (2015) http://dx.doi.org/10.1155/2015/232741.
[10] M.A. Nawi, Y.S. Ngoh, S.M. Zain, Photoetching of immobilized TiO_2-ENR50-PVC composite for improved photocatalytic activity, Int. J. Photoenergy, 12 (2012) http://dx.doi.org/10.1155/2012/859294.
[11] Y.S. Ngoh, M.A. Nawi, Fabrication and properties of an immobilized P25 TiO_2-montmorillonite bilayer system for the synergistic photocatalytic-adsorption removal of methylene blue, Mater. Res. Bull., 76 (2016) 8–21.
[12] W.I. Nawawi, R. Zaharudin, M.A.M. Ishak, K. Ismail, A. Zuliahani, The preparation and characterization of immobilized TiO_2/PEG by using DSAT as a support binder, Appl. Sci., 7 (2017) 24.
[13] R.A. Rashid, A.H. Jawad, M.A.M. Ishak, N.N. Kasim, KOH-activated carbon developed from biomass waste: adsorption equilibrium, kinetic and thermodynamic studies for methylene blue uptake, Desal. Water Treat., 57(56) (2016) 27226–27236.
[14] A.H. Jawad, R.A. Rashid, R.M.A. Mahmuod, M.A.M. Ishak, N.N. Kasim, K. Ismail, Adsorption of methylene blue onto coconut (*Cocos nucifera*) leaf: optimization, isotherm and kinetic studies, Desal. Water Treat., 57(19) (2016) 8839–8853.
[15] A.H. Jawad, R.A. Rashid, M.A.M. Ishak, L.D. Wilson, Adsorption of methylene blue onto activated carbon developed from biomass waste by H_2SO_4 activation: kinetic, equilibrium and thermodynamic studies, Desal. Water Treat., 57(52) (2016) 25194–25206.
[16] A.H. Jawad, S. Sabar, M.A.M. Ishak, L.D. Wilson, S.S.A. Norrahma, M.K. Talari, A.M. Farhan, Microwave-assisted preparation of mesoporous-activated carbon from coconut (*Cocos nucifera*) leaf by H_3PO_4 activation for methylene blue adsorption, Chem. Eng. Commun., 204 (2017) 1143–1156.
[17] H. Cherifi, S. Hanini, F. Bentahar, Adsorption of phenol from wastewater using vegetal cords as a new adsorbent, Desalination, 244 (2009) 177–187.
[18] H. Demir, A. Top, D. Balköse, S. Ülkü, Dye adsorption behavior of Luffa cylindrica fibers, J. Hazard. Mater., 153 (2008) 389–394.
[19] A. Dabrowski, P. Podkoscielny, M. Hubicki, M. Barczak, Adsorption of pheno- lic compounds by activated carbon—a critical review, Chemosphere, 58 (2005) 1049–1070.
[20] M. Boumediene, H. Benaïssa, B. George, S. Molina, A. Merlin, Characterization of two cellulosic waste materials (orange and almond peels) and their use for the removal of methylene blue from aqueous solutions, Maderas. Ciencia y Technologia, 17(1) (2015) 69–84.
[21] G. Annadurai, R.-S. Juang, D.-J. Lee, Use of cellulose-based wastes for adsorption of dyes from aqueous solutions, J. Hazard Mater., 92(3) (2002) 263–274.
[22] A.H. Jawad, N.F.H. Mamat, M.F. Abdullah, K. Ismail, Adsorption of methylene blue onto acid-treated mango peels: kinetic, equilibrium and thermodynamic study, Desal. Water Treat., 59 (2017) 210–219.
[23] S.X. Hou, Adsorption properties of pomelo peels against methylene blue dye wastewater, Adv. Mater. Res., 634–638 (2013) 178–181.
[24] A. Saeed, M. Sharif, M. Iqbal, Application potential of grapefruit peel as dye sorbent: Kinetics, equilibrium and mechanism of crystal violet adsorption, J. Hazard Mater., 179(1–3) (2010) 564–572.
[25] A. Bhatnagar, E. Kumar, A.K. Minocha, B.-H. Jeon, H. Song, Y.-C. Seo, Removal of anionic dyes from water using *Citrus limonum* (Lemon) peel: equilibrium studies and kinetic modeling, Separ. Sci. Technol., 44(2) (2009) 316–334.
[26] K. Amela, M.A. Hassen, D. Kerroum, Isotherm and kinetic study of biosorption of cationic dye onto banana peel, Energy Procedia., 19 (2012) 286–295.
[27] F. Moubarak, R. Atmani, I. Maghri, M. Elkouali, M. Talbi, M. Latifa, Elimination of methylene blue dye with natural adsorbent ''banana peels powder'', Glob. J. Sci. Front. Res. B Chem., 14 (2014)39–44.
[28] B.H. Hameed, Removal of cationic dye from aqueous solution using jackfruit peel as non-conventional low-cost adsorbent, J. Hazard Mater., 162(1) (2009) 344–350.
[29] B.H. Hameed, H. Hakimi, Utilization of durian (*Durio zibethinus Murray*) peel as low cost sorbent for the removal of acid dye from aqueous solutions, Biochem. Eng. J., 39(2) (2008) 338–343.
[30] F.A. Pavan, A.C. Mazzocato, Y. Gushikern, Removal of methylene blue dye from aqueous solutions by adsorption using yellow passion fruit peel as adsorbent, Bioresour. Technol., 99(8) (2008) 3162–3165.
[31] F.A. Pavan, E.C. Lima, S.L.P. Dias, A.C. Mazzocato, Methylene blue biosorption from aqueous solutions by yellow passion fruit waste, J. Hazard Mater., 150 (2008) 703–712.
[32] A. Bhatnagar, M. Sillanpaa, A. Witek-Krowiak, Agricultural waste peels as versatile biomass for water purification – A review, Chem. Eng. J., 270 (2015) 244–271.
[33] M.R. Moghadam, N. Nasirizadeh, Z. Dashti E. Babanezhad, Removal of Fe (II) from aqueous solution using pomegranate peel carbon: equilibrium and kinetic studies, Inter. J. Indust. Chem., 4 (2013) 19.
[34] M.V. Lopez-Ramon, F. Stoeckli, C. Moreno-Castilla, F. Carrasco-Marin, On the characterization of acidic and basic surface sites on carbons by various techniques, Carbon, 27 (1999) 1215–1221.
[35] W. Liu, Y. Liu, Y. Tao, Y. Yu, H. Jiang, H. Lian, Comparative study of adsorption of Pb(II) on native garlic peel and mercerized garlic peel, Environ. Sci. Pollut. Res., 21 (2014) 2054–2063.

[36] R. Dod, G. Banerjee, S. Saini, Adsorption of methylene blue using green pea peels (Pisum sativum): a cost-effective option for dye-based wastewater treatment, Biotechnol, Bioprocess Eng., 17 (2012) 862–874.
[37] A. Pattiya, J. O. Titiloye, A.V. Bridgwater, Fast pyrolysis of agricultural residues from cassava plantation for bio-oil production, Asian J. Energ. Environ., 8 (2007) 496–502.
[38] R. Xu, L. Ferrante, C. Briens, F. Berruti, Bio-oil production by flash pyrolysis of sugarcane residues and post treatments of the aqueous phase, J. Anal. Appl. Pyrol., 91 (2011) 263–272.
[39] N. Sellin, B.G. De Oliveira, C. Marangoni, O. Souza, A.P.N. De Oliveira, T.M. Novais De Oliveira, Use of banana culture waste to produce briquettes, Chem. Eng. Trans., 32 (2013) 349–354.
[40] N. Abdullah, F. Sulaiman, M.A. Miskam, R.M. Taib, Characterization of Banana (*Musa spp.*) Pseudo-Stem and Fruit-Bunch-Stem as a Potential Renewable Energy Resource. Inter. J. Biolog., Veteri, Agricul. Food Eng., 8 (2014) 712–716.
[41] O. Üner, Ü. Geçgel, Y. Bayrak, Preparation and characterization of mesoporous activated carbons from waste watermelon rind by using the chemical activation method with zinc chloride, Arab J. Chem., (2015) doi: http://dx.doi.org/10.1016/j.arabjc.2015.12.004.
[42] B.H. Hameed, M.I. El-Khaiary, Removal of basic dye from aqueous medium using a novel agricultural waste material: Pumpkin seed hull, J. Hazard Mater., 155(3) (2008) 601–609.
[43] C. Deng, J. Liu, W. Zhou, Y.K. Zhang, K.F. Du, Z.M. Zhao, Fabrication of spherical cellulose/carbon tubes hydrid adsorbent anchored with welan gum polysaccharide and its potential in adsorbing methylene blue, Chem. Eng. J., 200–202 (2012) 452–458.
[44] S. Senthilkumaar, P.R. Varadarajan, K. Porkodi, C.V. Subbhuraam, Adsorption of methylene blue onto jute fiber carbon: kinetics and equilibrium studies, J. Colloid Interface Sci., 284 (2005) 78–82.
[45] I. Langmuir, The adsorption of gases on plane surfaces of glass, mica and platinum, J. Am. Chem. Soc., 40(9) (1918) 1361–1403.
[46] F. Gimbert, N. Morin-Crini, F. Renault, P.-M. Badot, G. Crini, Adsorption isotherm models for dye removal by cationized starch-based materials in a single component system: Error analysis, J. Hazard Mater., 157(1) (2008) 34–46.
[47] H.M.F. Freundlich, Over the adsorption in solution, J. Phys. Chem., 57 (1906) 385–470.
[48] T.W. Weber, R.K. Chakravorti, Pore and solid diffusion models for fixed bed adsorbers, AlChE J., 20(2) (1974) 228–238.
[49] K.Y. Foo, B.H. Hameed, Preparation, characterization and evaluation of adsorptive properties of orange peel based activated carbon via microwave induced K_2CO_3 activation, Bioresour. Technol., 104 (2012) 679–686.
[50] B.H. Hameed, A.T.M. Din, A.L. Ahmad, Adsorption of methylene blue onto bamboo-based activated carbon: Kinetics and equilibrium studies, J. Hazard Mater., 141(3) (2007) 819–825.
[51] S. Lagergren, About the theory of so called adsorption of soluble substances, kungl. Svenska Vetenskapsakademien, Handlingar, Band, 24(4) (1898) 1–39.
[52] Y.S. Ho, G. McKay, Pseudo-second order model for sorption processes, Process Biochem., 34 (1999) 451–465.
[53] O. Hamdaoui, Batch study of liquid-phase adsorption of methylene blue using cedar sawdust and crushed brick, J. Hazard Mater., 135 (1–3) (2006) 264–273.
[54] F.M. Machado, C.P. Bergmann, E.C. Lima, B. Royer, F.E. de Souza, I.M. Jauris, T. Calvete, S.B. Fagan, Adsorption of Reactive Blue 4 dye from water solutions by carbon nanotubes: experiment and theory, Phys. Chem. Chem. Phys., 14(31) (2012) 11139–11153.